

1 Summaries of Experimental Activities

1.1 E08-027

A. Camsonne, J.P. Chen, D. Crabb, K. Slifer, spokespersons,
and
the Hall A Collaboration.
contributed by R. Zielinski

1.1.1 Motivation

The inclusive scattering spin structure function (SSF) g_2^p is largely unmeasured at low and moderate Q^2 values; the lowest momentum transfer that has been investigated is 1.3 GeV^2 by the RSS collaboration [2]. Poor knowledge of g_2^p , along with the other SSFs (g_1^n , g_2^n , and g_1^p), in the low Q^2 region is now a limiting factor in the precision of bound-state QED calculations. The finite size of the nucleon, as characterized by the structure functions has become the leading uncertainty. Furthermore researchers from PSI [1] have obtained a value for the proton charge radius $\langle R_p \rangle$ via measurements of the Lamb shift in muonic hydrogen, which differs significantly from the value from elastic electron proton scattering. The main uncertainties in the PSI results originate from the proton polarizability and from different values of the Zemach radius. These quantities are determined from integrals of the SSF and elastic form factors, which due to kinematic weighting, are dominated by the low Q^2 region.

The existing data has also revealed a striking discrepancy [3] of χ PT calculations with the longitudinal-transverse polarizability δ_{LT}^p . This is surprising since δ_{LT} was expected to be a good testing ground for the chiral dynamics of QCD [4, 5] due to its relative insensitivity to resonance contributions. Measurement of g_2^p at low Q^2 will give access to δ_{LT}^p and allow an isospin examination of this ‘ δ_{LT} puzzle’.

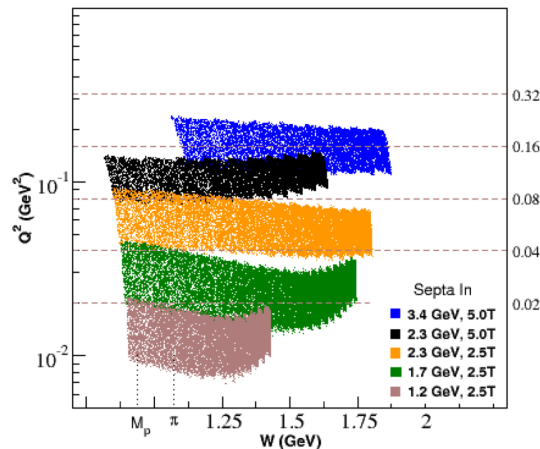


Figure 1: Kinematics covered during experimental run period. The right-hand side vertical axis is the extrapolation to constant Q^2 . As W increases (and momenta decreases) Q^2 rises due to the target field creating a larger scattering angle.

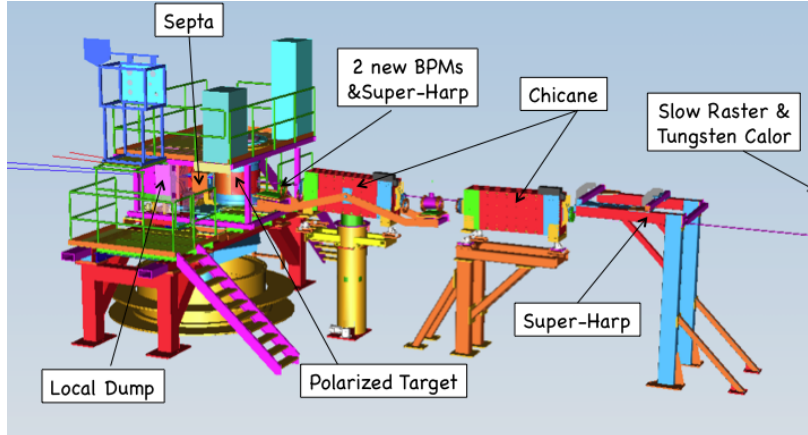


Figure 2: E08-027 installation in Hall A. The third arm detector was located on the left hand side of the bottom target-platform.

1.1.2 The Experiment

The experiment successfully ran March - May 2012 (see Table 1). We performed an inclusive measurement at forward angle of the proton spin-dependent cross sections in order to determine the g_2^p structure function and the longitudinal-transverse spin polarizability δ_{LT} in the resonance region for $0.02 < Q^2 < 0.20 \text{ GeV}^2$ (See Figure 1). To reach the lowest possible momentum transfer, a pair of room temperature septa magnets were installed to allow detection of scattered electrons at 5.69° . During the run period the right spectrometer (RHRS) septa magnet was damaged twice. After each incident magnet coils were bypassed, limiting its field strength and momenta range. Dynamical Nuclear Polarization (DNP) was used to polarize the solid ammonia target. The original target's superconducting magnet coil was damaged during testing, but a similar target was successfully transplanted from Hall B and used during the experiment.

Table 1: Statistics of kinematic settings taken during run period. Running was split between 2.5 T and 5.0 T target field strength configurations. At lower beam energies (and lower momenta) the 5.0 T target field effectively increased the scattering angle of the detected electrons. This would have limited our low Q^2 range. To fix this, 2.254 GeV, 1.704 GeV and 1.158 GeV were all run with the target field at half-strength, 2.5T.

$E_0(\text{GeV})$	Target (T)	Recorded Triggers
2.254	2.5	3.80E+09
1.706	2.5	3.20E+09
1.158	2.5	4.00E+09
2.254	5.0	7.00E+08
3.352	5.0	4.00E+08

The DNP target's strong magnetic field required the installation of two large FZ magnets upstream of the target to provide chicaning of the beam (see Figure 2). In order to limit depolarization of the polarized ammonia target the experiment ran low currents ($\sim 50 - 100 \text{ nA}$), which required the installation of two new super-harps and two new M15 antennae style beam position monitors (BPMs) to fully characterize the beam profile. To further minimize depolarization a slow raster was installed to raster the beam over the entire $\sim 2 \text{ cm}$ diameter target cup. The lower beam currents also led to the installation of a low current tungsten calorimeter to calibrate the beam current monitors (BCMs).

A new third arm detector was designed for the experiment to give a relative measurement of the combination of beam and target polarization at a 10% level. The detector counted the elastic recoil proton at

large scattering angle in order to measure the elastic proton asymmetry. This asymmetry is related to the beam and target polarization. It was installed on beam left at an angle of approximately 70° .

1.1.3 Experimental Progress

A Geant4 based program was developed to simulate the the physics for the high resolution spectrometers (HRS) together with the target and septum fields. The full geometries of the experimental setup have been built in (see Figure 2). This includes the chicane fields for each kinematic setting as well as the two target field configurations and several versions of the septum fields which are varied in the number of active coils in the right septum. The optics run plan was determined based on the simulation; we will use it to improve optics calibration and determine the spectrometer acceptance.

Currently spectrometer optics data has been optimized for no target field, chicane set to straight-through running on both the left and right HRS. Straight-through optimization removes the added complexity of the target field and allows for an optics calibration focusing on the septa and HRS magnets. The angle calibration results of the left-HRS straight-through setting are shown in Figure 3. Momentum matrix elements have also been calibrated. Work has now shifted to repeating the same analysis but with a longitudinal target field. The next step is to then determine the optics for the production settings with a transverse target field at both 2.5 T and 5.0 T. The effect of the different right-HRS septa coil packages on the optics for both left and right spectrometer optics is also being analyzed.

Beam position information is also needed for the optics optimization. The straight-through calibration of the BPMs is finished; a new method was created to calculate the beam position from the four-antenna BPMs. The BPM analysis package also includes a transfer function from the BPMs to the target, taking into account the 2.5 T and 5.0 T target fields. The current analysis effort is to create this transfer function. We are also looking into the non-linearity of the slow raster and the issue of increased noise in the BPM signal for low-current running.

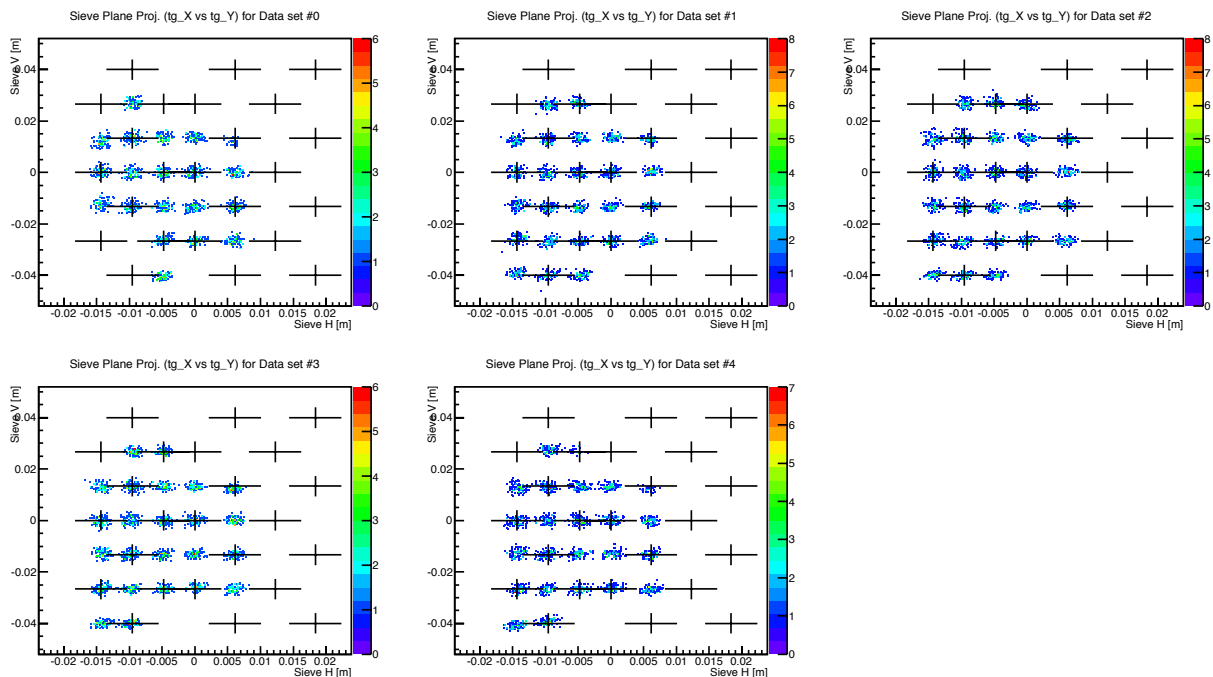


Figure 3: Sieve slit pattern: X vs. Y. Each cross represents the position of the sieve hole used to calibrate the theta and phi angles. The events from each sieve hole have been aligned well as a sieve pattern is clearly visible. Five panels represent different delta scan runs, which together represent the focal plane momentum coverage, -3.5%, -2%, 0, 2%, 3.5%, respectively.

Spectrometer detector efficiencies are needed as a correction to the measured cross section. A first round calibration of the HRS detectors is now finished. This includes particle identification (PID) calibrations on the gas Čerenkov and lead glass on both spectrometer arms. Detector and cut efficiency analysis on the PID detectors is currently underway. The S1 and S2m trigger scintillator efficiency is also finished for both arms. The results for the left-HRS are shown in Figure 4. The trigger efficiency for all good production runs is above 99%.

An electron asymmetry measurement is needed along with the absolute cross-section to extract δ_{LT}^p . To make the asymmetry measurement, beam helicity information was needed. The experiment used the helicity scheme set by Qweak, which was also used in the DVCS experiment. Although we required a higher trigger rate in the data acquisition (DAQ) system. The g_2^p helicity decoder package is a combination of the DVCS and normal Hall A decoders. The package has already been tested during the production running and worked well with very preliminary asymmetries calculated during the production run period.

Target polarization measurement is also needed to determine an asymmetry. The calibration constants, used to convert the NMR signal into a polarization, for all target materials and settings have been calculated. They can now be applied to the polarization signals on a run by run basis to obtain averaged target polarizations with relative uncertainties in the 1-4% range. Still to be done is a quality check of the target NMR signal throughout the experiment, along with some polarization signal fit adjustments to reduce uncertainties.

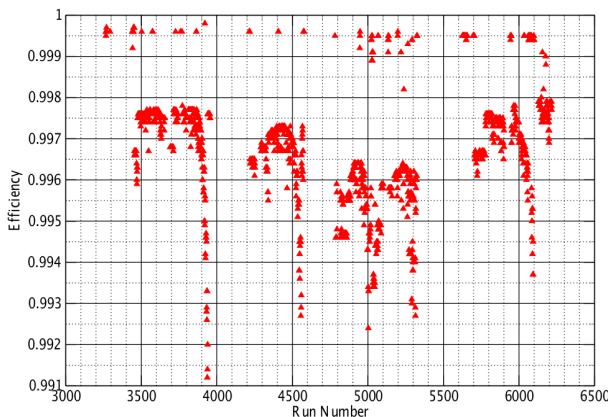


Figure 4: Left-HRS trigger efficiency results for all production runs.

Following the completion of the target analysis, base optics and BPM calibrations, and first round detector calibrations, the experiment is beginning to move into first-pass farm production. Optics will continue with the effort moving to optimization of the production settings, and the BPM calibrations for the same settings. The GEANT simulation will also be used to begin work on determining the experimental acceptance needed for a cross section measurement. The detector efficiencies will be finalized and we will start the asymmetry-dilution analysis which determines what percentage of the electrons detected by the HRS were not scattered off of a proton from the ammonia target.

References

- [1] R. Pohl *et al.*, Nature **466**, 213 (2010).
- [2] F. R. Wesselmann *et al.* [RSS Collaboration], Phys. Rev. Lett. **98**, 132003 (2007).
- [3] M. Amarian *et al.* [Jefferson Lab E94010 Collaboration], Phys. Rev. Lett. **93**, 152301 (2004).
- [4] V. Bernard, T. R. Hemmert and U. G. Meissner, Phys. Lett. B **545**, 105 (2002).
- [5] C. W. Kao, T. Spitzenberg and M. Vanderhaeghen, Phys. Rev. D **67**, 016001 (2003).